Sensors and Materials, Vol. 38, No. 3 (2026) 1717–1730
MYU Tokyo

S & M 4402

Acoustic–Vibration Fusion with Sparse Representation for Intelligent Fault Detection in Home Appliances

Yuchao Zhao[1] and Zhengji Mao[2*]

[1]School of Information Engineering, Xiamen Ocean Vocational College,
No. 4566 Hongzhong Avenue, Xiamen City, Fujian 361100, P. R. China
[2]School of Marine Mechatronics, Xiamen Ocean Vocational College,
No. 4566 Hongzhong Avenue, Xiamen City, Fujian 361100, P. R. China

(Received January 29, 2026; accepted March 9, 2026)

Keywords: fault diagnosis, sound and vibration, adaptive feature fusion, sparse representation

The increasing complexity of home appliances necessitates robust fault detection systems to ensure operational safety and reduce maintenance costs. Therefore, we developed an acoustic–vibration fusion framework based on sparse representation (AVF-SR) to enable intelligent fault monitoring in home appliances. By integrating contact-based vibration sensors (accelerometers) and noncontact acoustic sensors (micro-electro-mechanical system microphones), AVF-SR overcomes the limitations of single-modality systems in noisy household environments. In AVF-SR, we used multiscale wavelet decomposition and an adaptive feature fusion mechanism based on the Fisher Discrimination Criterion to adjust sensor weights according to appliance state. The experimental results on a drum-type washing machine, a split-type air conditioner, and a refrigerator demonstrated that adaptive fusion improves identification accuracy by 15 to 25% compared with those of static weighting methods. SR enhanced recognition accuracy from 65 to over 85% even under low signal-to-noise ratio (–5 dB) conditions. Diagnostic confidence scores ranged from 0.72 to 0.85. The results of this study provide a basis for the development of advanced, lightweight sensors for deployment on low-power microcontrollers in consumer electronics. The limitations of this study related to fault types and laboratory-controlled simulations necessitate further research to enhance model generalizability across diverse appliances and investigate self-supervised learning, which addresses the scarcity of labeled fault data in home appliance deployments.

1. Introduction

The increasing complexity and embedded intelligence of modern home appliances necessitate the development of robust, automated condition monitoring and fault detection systems. The early and accurate identification of incipient faults, such as bearing wear, rotor imbalance, and structural loosening, is essential for preventing unexpected failures, ensuring user safety, and reducing maintenance costs. However, existing fault diagnosis methods rely on manual

*Corresponding author: e-mail: maozhengji@xmoc.edu.cn
https://doi.org/10.18494/SAM6246

ISSN 0914-4935

inspection or single-sensor data analysis, presenting limitations when applied to the noisy and variable operating conditions of household devices. The methods applied to home appliances for early fault detection suffer from low sensitivity and high false-alarm rate and cannot generalize across different appliances or diverse usage patterns.

To enhance the reliability of faults in these environments, recent diagnostic systems adopt a combination of contact and noncontact sensors to capture the mechanical state of the appliance. Vibration sensors, typically piezoelectric accelerometers, are mounted to the internal structure to capture high-frequency mechanical shocks and structural resonances. While these sensors are effective at isolating internal defects from ambient noise, they are limited to point-contact measurements. To complement this, acoustic sensors, such as MEMS microphones, are used to capture airborne sound signatures. Microphones provide a noncontact sensing solution that can detect faults manifested as high-frequency hissing or whining, which might not be strongly transmitted through the chassis. Table 1 shows the sensors commonly utilized in fault diagnosis.

Researchers have proposed data-driven intelligent fault detection methods that leverage these acoustic and vibration signals to identify symptoms such as bearing wear, rotor imbalance, and structural loosening. The synergy between these two signal types is a well-established foundational approach for gear fault classification,[3,4] providing essential data for detecting bearing defects and diagnosing complex composite faults.[4,5] Recently, low-rank modeling has been adopted to isolate fault signatures from complex, noisy environments. This mathematical method represents data within a low-dimensional subspace, where mechanical faults are treated as sparse deviations from a healthy low-rank baseline. This principle has been effectively implemented in adaptive tensor models[4] and remains a core component of research into weak fault extraction.[6]

In parallel, time-frequency analysis and deep learning are also integrated for fault detection. By converting one-dimensional signals into two-dimensional representations using techniques such as the short-time Fourier transform or continuous wavelet transform, advanced computer vision architectures are utilized for fault detection. Specifically, Vision Transformers (ViTs) have demonstrated superior performance in classifying faults on the basis of these time-frequency representations.[7,8] To further refine feature extraction, hybrid models such as Convolutional Neural Networks (CNN)–ViT architectures are widely applied to integrate local feature learning with global context modeling.[8,9]

Despite these advancements, high-performance deep learning models are computationally

Table 1
Sensors used in fault diagnosis.

Sensor	Parameter	Advantage	Limitation
Piezoelectric accelerometer[1]	Structural vibration (m/s^2)	High sensitivity to internal mechanical shocks, immune to ambient noise.	Requires rigid mounting, limited to point-contact measurements
MEMS microphone[2]	Airborne sound pressure (pascal)	Noncontact installation, capturing high-frequency whining or hissing	Highly susceptible to external environmental noise (voices or televisions)
Current/voltage sensors	Electrical signatures	Detecting electrical motor faults (winding shorts)	Indirect indicator of mechanical health, poor for structural loosening

expensive and require massive datasets, which is challenging for widespread deployment on the cost-sensitive, low-power microcontrollers of consumer appliances. When fault data are insufficient, digital twin (DT) technology is used to address the data scarcity by generating high-fidelity synthetic datasets,[10] or novel sensing systems are used to capture airborne sound effectively.[11] Model generalizability under various conditions is also enhanced through domain adaptation,[12,13] anomaly detection methods,[13] and lightweight models for edge-level computation.[14,15] Recently, acoustic–vibration data integration has been adopted for motor fault diagnosis[16] to address the inherent limitations of single-modality systems.

In this study, we developed an acoustic–vibration fusion framework with sparse representation (AVF-SR) for intelligent fault detection in home appliances. The framework acquires vibration and audio signals, extracts sparse features from each modality using learned dictionaries, and fuses these features into a compact yet informative indicator for fault detection. This method improves detection accuracy by leveraging complementary sensor data and enhances robustness against household noise through sparse denoising. Furthermore, AVF-SR enables efficient deployment in cost-sensitive consumer products by maintaining a lightweight computational footprint. The framework was validated through experiments on a drum-type washing machine, where it demonstrated superior fault detection ability and stronger resilience to background noise than single-modality baseline methods.

The results of this study provide a basis for the development of advanced, lightweight sensors for deployment on low-power microcontrollers in consumer electronics. The developed AVF-SR framework does not merely serve as an analytical tool but establishes a novel sensing concept for multimodal data integration in consumer electronics. By defining the adaptive weighting requirements for acoustic and vibration signals, in this study, we provide a roadmap for the development of integrated, multifunctional sensor chips that adjust their sensitivity and power consumption on the basis of the detected operational state. Such advancements are critical for the next generation of ‘intelligent’ sensors capable of onboard processing.[17]

2. Methodology

2.1 Data collection

AVF-SR employs the following procedure (Fig. 1): First, sound and vibration signals from the target home appliance are collected. Multiscale wavelet decomposition is applied separately to each modality, producing the corresponding wavelet coefficients. Features are extracted from these coefficients and subsequently fused to form a combined feature set. Sparse representation is applied to the fused features, yielding a refined representation that enhances robustness. Finally, the enhanced features are compared with a preestablished fault feature library to identify the fault type and determine its location within the appliance.

In this study, sound and vibration signals were acquired from the appliance under inspection. Sound data were recorded using a built-in microphone sampled at 44.1 kHz to capture the full range of audible frequencies, while vibration signals were obtained through a MEMS accelerometer sampled at 1 kHz. The duration of data collection depended on the appliance type:

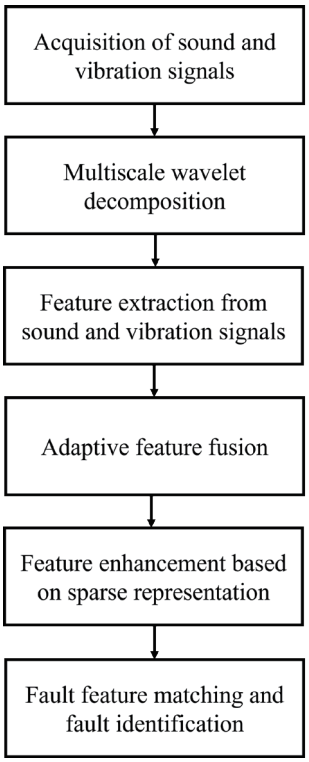

Fig. 1. Workflow of AVF-SR developed in this study.

for a drum-type washing machine, one full washing cycle or 3–5 min of representative operation; for an air conditioner, 3 min after stable operation; and for a refrigerator, 1–2 min of recording. Sensor placement was essential to ensure data quality. The microphone was positioned within 30 cm of the appliance, and the vibration sensor was mounted directly onto the housing, preferably near critical components such as bearings, motors, or mounting points. The signals were digitized and verified for quality by assessing their time-domain waveforms and signal-to-noise ratios to ensure they adequately captured the unique operational fingerprints of each appliance.[18]

The data collected underwent multiscale wavelet decomposition of the sound and vibration. This method was used to replace conventional Fourier-based analysis, processing the transient and nonstationary signal patterns typically found in home appliance fault signals.

2.2 Data processing

The data were processed to convert heterogeneous sensor data into discriminative indicators of faults through multiscale decomposition, adaptive fusion, and sparse enhancement.

2.2.1 Multiscale signal decomposition and preprocessing

The acoustic (sampling frequency, f_s = 44.1 kHz) and vibration (f_s = 1 kHz) signals are segmented into overlapping windows of 2048 and 1024 points, with a 50% overlap to mitigate spectral leakage. To ensure optimal signal characterization, a wavelet basis function is selected from Daubechies (db4–db20), Symlets (sym4–sym8), or Coiflets (coif1–coif5) families by minimizing the reconstruction error.

$$E_{recon} = \sqrt{\frac{\sum_{i=1}^{N}\left(x_i - \hat{x}_i\right)^2}{N}}\,. \tag{1}$$

Here, x_i and $\hat{x}_i$ represent the original and reconstructed sampling points, respectively.[19]

Acoustic signals undergo a five-level decomposition from 689 to 11025 Hz, while vibration signals are decomposed into 7 levels from 3.9 to 500 Hz. This multiscale decomposition is defined as.

$$x(t) = \sum_{j=1}^{J}\sum_{k} d_j[k]\psi_{j,k}(t) + \sum_{k} a_J[k]\phi_{J,k}(t)\,. \tag{2}$$

Here, $x(t)$ is the input signal as a function of time t, $d_j[k]$ represents the detailed coefficients at the jth level and the kth position, $a_J[k]$ denotes the approximation coefficients at the Jth level and the kth position, $\psi_{j,k}(t)$ is the wavelet function at scale j and translation k, $\phi_{J,k}(t)$ is the scaling function at the maximum decomposition level J and translation k, J is the maximum decomposition level (set to 5 for sound signals and 7 for vibration signals), j is the decomposition level index, ranging from 1 to J, and k is the position index, which depends on the signal length.

2.2.2 Feature extraction and adaptive Fisher fusion

From the resulting wavelet coefficients, four feature categories are extracted: energy distribution, statistical moments (kurtosis, skewness, mean, and standard deviation), peak characteristics, and energy entropy. The energy percentage E_j for the jth layer is calculated to identify frequency-specific anomalies.

$$E_j = \frac{\sum_k \left|d_j[k]\right|^2}{\sum_{j=1}^{J}\sum_k \left|d_j[k]\right|^2 + \sum_k \left|a_J[k]\right|^2} \times 100\% \tag{3}$$

Here, E_j is the energy percentage of the wavelet coefficients of the jth layer, $d_j[k]$ is the detailed coefficient of the jth layer at the kth position, $a_J[k]$ is the approximation coefficient of the Jth layer at the kth position, j is the decomposition layer index, ranging from 1 to J, J is the

maximum number of decomposition layers, k is the position index, which depends on the signal length, and $|\cdot|$ represents the absolute value operation.

To integrate the resulting 84-dimensional feature set (35 acoustic and 49 vibration), we employ an adaptive fusion mechanism based on the Fisher Discrimination Criterion.[20] The discriminative score d_i for each feature is determined by the ratio of interclass distribution (S_b) to intraclass distribution (S_w).

$$d_i = \frac{S_b^i}{S_w^i} \tag{4}$$

Here, d_i is the discriminative score of the ith feature, S_b^i is the interclass distribution of the feature, S_w^i is the intraclass distribution of the feature, and i is the feature index. S_b^i and S_w^i are determined using Eqs. (5) and (6), respectively.

$$S_b^i = \sum_{c=1}^{C} n_c \left(\mu_c^i - \mu^i \right)^2 \tag{5}$$

$$S_w^i = \sum_{c=1}^{C} \sum_{j \in c} \left(x_j^i - \mu_c^i \right)^2 \tag{6}$$

Here, C is the total number of fault categories, n_c is the number of samples in the cth class, μ_c^i is the mean of the cth class samples on the ith feature, μ^i is the mean of all samples on the ith feature, x_j^i is the value of the jth sample on the ith feature, c is the class index, ranging from 1 to C, and $j \in c$ represents all samples j belonging to the cth class.

Feature weights $w_i(t)$ are adjusted using a learning rate α and a device-specific time-adjustment function $f(t,T)$ to prioritize vibration data during high-load cycles (e.g., washing machine spinning) or acoustic data during stable operation. The experimental results indicated that this adaptive weighting improves identification accuracy by 15 to 25% compared with that of static fusion methods.

2.2.3 Sparse representation and fault recognition

The fused feature vector is refined using SR to suppress environmental noise and amplify fault-specific signatures. An over-complete dictionary D is constructed, consisting of atomic vectors representing healthy and various fault states (inner or outer bearing defects). The enhanced feature vector Y is reconstructed using optimized sparse coefficients $\hat{\alpha}$.

$$Y = D\hat{\alpha} \tag{7}$$

By utilizing sparse denoising, AVF-SR maintains high recognition accuracy (>85%) even at low signal-to-noise ratios (–5 dB).[21] Final diagnosis is performed by evaluating the

reconstruction error e_c across subdictionaries. A confidence score is derived from the ratio of the minimum to the second-minimum error to determine the final diagnostic output.

$$Score = 1 - \frac{e_{min}}{e_{second\_min}} \tag{8}$$

Here, score denotes the confidence score, e_{min} is the minimum reconstruction error, and e_{second_min} is the second-minimum reconstruction error. A definitive diagnosis is issued when the score exceeds a calibrated threshold (0.3–0.5), ensuring a reliable and autonomous monitoring system for consumer appliances.

By employing this modular sensing and processing architecture, the system provides a robust solution for in-home appliance monitoring that aligns with current trends in intelligent sensor data integration.

3. Results

To validate the performance of AVF-SR, three home appliances were used, namely, a washing machine, an air conditioner, and a refrigerator (Fig. 2, Table 2). The experiment was conducted on three household appliances with various service histories to ensure the evaluation of the sensing framework. The drum-type washing machine and the refrigerator were used for 4 and 7 years, respectively, with natural mechanical wear. The split-type air conditioner was used for a year, where specific fault conditions were simulated by adding calibrated weights to the fan

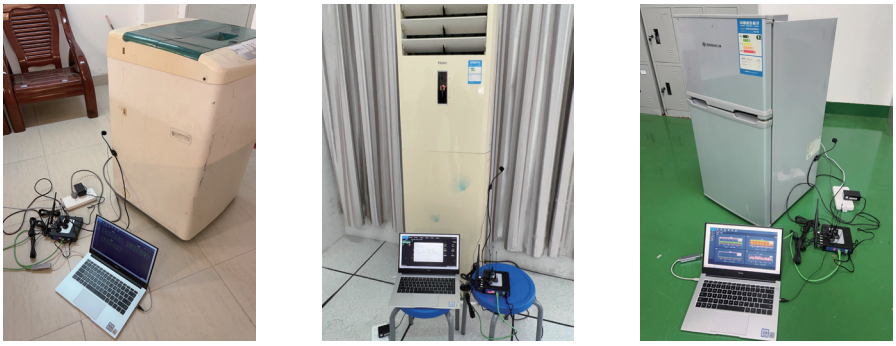

(a) (b) (c)

Fig. 2. (Color online) Home appliances used in our experiment: (a) washing machine, (b) air conditioner, and (c) refrigerator.

Table 2
Specifications of home appliances used in our experiment.

Feature	Washing machine	Air conditioner	Refrigerator
Type	Front load	Split-system inverter	Double door
Average power	2000 W (with heating)	1000 W	200 W
Voltage	220–240 V	220–240 V	220–240 V
Load type	Inductive	Inductive	Inductive

blades to simulate imbalance. This method allows the framework to be tested for the stochastic nature of wear and known failure modes.[22]

3.1 Signal characteristics and waveform analysis

To demonstrate the validity of the data acquisition system, raw waveforms for the acoustic and vibration signals of the drum-type washing machine were obtained as shown in Fig. 3. The vibration signal, captured by the mounted accelerometer at 1 kHz, exhibits clear periodic impulses corresponding to the mechanical rotation and structural shocks of the spin cycle. In contrast, the acoustic signal, sampled at 44.1 kHz, shows a higher-frequency distribution comprising motor whining and transient noise from water movement. These distinct signatures confirm that the integrated sensors effectively capture the multimodal operational state of the appliance.[18]

3.2 Washing machine bearing fault

A drum-type washing machine was operated under a high-load spinning cycle. Vibration and sound signals were collected over a complete washing cycle (3–5 min). During this phase, the feature weight was adjusted to 0.7 for vibration, consistent with the principle of prioritizing structural sensors during high-intensity mechanical operation. The multiscale wavelet decomposition result revealed a significant increase in high-frequency energy in the first two wavelet layers, accompanied by a high kurtosis value. The fusion module assigned a weight of 0.7 to vibration features. After sparse representation enhancement, AVF-SR matched the extracted features with the fault library. The analysis results showed the early-stage wear of the inner race of the bearings with a confidence score of 0.85 (Table 3). The results indicated the necessity of bearing replacement to prevent further mechanical degradation. This result demonstrates the effectiveness of multiscale wavelet decomposition in isolating high-frequency mechanical shocks from the noisy environment of a rotating drum.

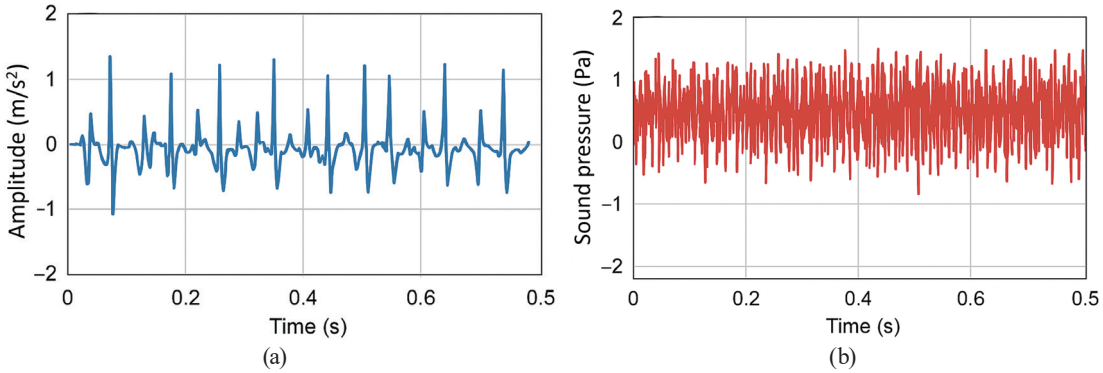

Fig. 3. (Color online) Time-domain waveforms for drum-type washing machine during spin cycle: (a) vibration signal (f_s = 1 kHz) and (b) acoustic signal (f_s = 44.1 kHz).

Table 3
Experimental results for washing machine.

Category	Detail
Sensing method	Microphone placed on top during operation
Signal type/frequency	High-frequency vibration
Wavelet layer	Layers 1 and 2
Signal analysis technique	Multiscale wavelet decomposition, sparse representation
Key indicators	Significant energy increase, kurtosis value higher than normal
Feature weight	0.7 for vibration
Identified fault	Early wear of inner ring of bearings
Confidence score	0.85
Recommendation	Replace bearings to prevent severe damage

3.3 Air conditioner fan imbalance

Data from the split-type inverter air conditioner were collected 3 min after the system reached stable operation, focusing on the indoor unit. To capture multimodal signatures of fan imbalance, a MEMS microphone was positioned within 30 cm of the unit to record airborne sound pressure, while an accelerometer was mounted on the housing near the blower motor to measure structural vibration. The sensors were used to detect high-frequency whining and mechanical resonances when vibrations were dampened by the plastic chassis. Being different from the washing machine experiment, which emphasized high-frequency noise (wavelet layers 1–2), the air conditioner analysis targeted mid-frequency components (layers 3–4), optimized for identifying the rotational harmonics of the blower fan. Periodic mid-frequency energy fluctuations and abnormal skewness were observed, both indicative of fan imbalance (Table 4).

Feature weight was assigned according to operational state. During startup, sound and vibration weights were balanced at 0.5, while during stable operation, the weight function $w_i(t)$ was adjusted to 0.6 for acoustic data. This prioritization reflects the diagnostic importance of airborne sound signals, such as whistling or humming, which indicate rotor imbalances that might not be transmitted through the plastic chassis to vibration sensors.

In AVF-SR, deviations in skewness and periodic energy fluctuations were treated as sparse anomalies relative to the healthy baseline, enabling fault isolation in household background noise. After feature enhancement, AVF-SR matched the extracted features to the fault library and identified an unbalanced fan impeller. Diagnostic confidence was quantified by the reconstruction error ratio, yielding scores of 0.72–0.78, both exceeding the calibrated threshold of 0.3–0.5. The results indicated the necessity of rotor alignment calibration or professional balancing to mitigate structural resonance and ensure long-term operational stability.

3.4 Refrigerator compressor relay fault

Data from the refrigerator were analyzed to evaluate the system's ability to detect electrical motor faults. The microphone was placed near the compressor during startup, capturing low-frequency sound signals. The analysis targeted wavelet layers 4–5, corresponding to the frequency of 689–2756 Hz (Table 5). This differs from the washing machine's high-frequency

Table 4
Experimental results for air conditioner.

Category	Detail
Sensing method	Microphone placed near indoor unit during operation
Signal type/frequency	Mid-frequency vibration
Wavelet layer	Layers 3 and 4
Signal analysis technique	Multi-scale wavelet decomposition, sparse representation
Key indicators	Periodic energy fluctuations, skewness value deviation
Feature weight	0.5 for startup, 0.6 for stabilized operation
Identified fault	Unbalanced fan impeller
Confidence score	0.72
Recommendation	Clean the fan impeller for balance adjustment

Table 5
Experimental results for refrigerator.

Category	Detail
Sensing method	Microphone placed near compressor during startup
Signal type/frequency	Low-frequency sound
Wavelet layer	Layers 4 and 5
Signal analysis technique	Multiscale wavelet decomposition, sparse representation
Key indicators	Abnormal energy distribution, multiple startup attempts
Feature weight	0.65 for sound
Identified fault	Faulty start relay
Confidence score	0.78
Recommendation	Replace starter relay

focus, as compressor startup issues typically manifest as low-frequency clicks or humming. Multiscale wavelet decomposition results revealed abnormal energy distribution across these layers, while repeated startup attempts were identified as sparse deviations from the healthy low-rank baseline. Feature weight was adjusted to prioritize acoustic data, with sound features assigned a weight of 0.65, reflecting the diagnostic importance of airborne sound, which a noncontact MEMS microphone captures more effectively than vibration sensors.

Energy percentage (E_j) was calculated for each layer to isolate frequency-specific anomalies during the transient startup phase. SR denoising enhanced recognition accuracy, enabling the system to distinguish fault-related signals from typical kitchen background noise. After feature enhancement, AVF-SR matched the extracted features to the fault library and diagnosed a faulty start relay. Diagnostic confidence was quantified by evaluating the reconstruction error (e_c) across fault subdictionaries, presenting a score of 0.78. Since this exceeds the calibrated threshold of 0.3–0.5, the results indicated the necessity of relay replacement to prevent further compressor startup failures.

4. Discussion

The experimental results validated AVF-SR as a robust methodology for the condition monitoring of home appliances. By integrating multiscale wavelet analysis, adaptive feature

fusion, and sparse representation, the system overcomes the limitations of single-modality sensing and high environmental noise.

The wavelet basis function captured the transient signals of each appliance. The Symlet wavelet was effective for the washing machine's spin cycle, where abrupt mechanical shocks from unbalanced loads require a wavelet that handles nonstationary signals. Conversely, the Daubechies wavelet (db8) and Coiflet wavelet (Coif5) were well suited for the steady compressor sounds of the air conditioner and the symmetrical startup patterns of the refrigerator motor.

Five decomposition levels for acoustic (689–11,025 Hz) and seven levels for vibration (3.9–500 Hz) were of sufficient resolution to isolate faults across different frequency bands. In high-frequency bands (layers 1–2), bearing wear in the washing machine was effectively isolated, where high kurtosis values implied sharp pulse signals typical of internal mechanical shocks. In mid-frequency bands (layers 3–4), rotor imbalances in the air conditioner blower fan were effectively isolated through skewness deviations. In low-frequency bands (layers 4–5), start relay failures in the refrigerator were detected, manifesting as low-frequency clicks or humming.

Fixed-weight sensing is insufficient for the variable operating states of household devices. The adaptive fusion mechanism, guided by the Fisher Discrimination Criterion, improved identification accuracy by 15 to 25% over static methods. In the washing machine, a 0.7 vibration weight was necessary during the high-load spin-drying phase to prioritize structural integrity. In the air conditioner, while startup required a balanced 0.5/0.5 weight, stable operation prioritized acoustic data (a 0.6 weight) to capture airborne whining that the plastic chassis might dampen. In the refrigerator, a 0.65 acoustic weight allowed the noncontact MEMS microphone to better capture the transient relay clicks during the critical startup phase.

The integration of SR is effective in overcoming household background noise, such as voices in conversation. By treating faults as sparse deviations from a healthy low-rank baseline, AVF-SR amplified unique fault signatures while suppressing redundancy. This was most evident in the refrigerator, where SR denoising enabled the distinction of a faulty start relay from kitchen background noise, maintaining high diagnostic confidence. AVF-SR demonstrated that SR boosted recognition accuracy from 65 to more than 85% even under low signal-to-noise ratio (–5 dB) conditions.

The final diagnostic confidence scores for the three appliances (0.85 for the washing machine, 0.72–0.78 for the air conditioner, and 0.78 for the refrigerator) exceeded the calibrated threshold of 0.3–0.5. This suggests that the AVF-SR framework provides a reliable, autonomous monitoring solution that is scientifically accurate and computationally efficient for deployment on cost-sensitive consumer electronics.

The AVF-SR framework developed in this study was designed for lightweight deployment on embedded microcontrollers commonly used in consumer appliances. The feature extraction and sparse representation modules were optimized to operate within the computational limits of Advanced Reduced Instruction Set Computing Machine Cortex-M series processors and similar low-power chips. In practice, vibration and acoustic sensors can be integrated into the appliance's control board, with real-time processing performed locally. Diagnostic results, including fault type and confidence score, can be communicated to users through the appliance's display panel, smartphone applications, or smart home ecosystems using Wi-Fi or Bluetooth. This integration

enables prompt fault notifications and actionable recommendations without requiring external PCs. Recent advances in edge AI and embedded sparse modeling support the feasibility of such integration.[23]

For the integration of the developed framework at household, the cost-effectiveness of fault detection is an important consideration. Traditional reactive maintenance occurs only after an appliance has failed, which might require repair costs for major components (a refrigerator compressor or washing machine motor) that exceed 50% of the cost of a new unit, leading consumers to favor replacement.[24] The developed AVF-SR framework enables predictive maintenance. By identifying early-stage acoustic and vibration anomalies, the framework alerts users to minor issues, such as fan imbalances or lubrication needs, that can be resolved at a reduced cost of a full replacement. For manufacturers, this sensing concept can be integrated into the warranty period for early defect detection, preventing the unexpected failure of components and reducing service costs.[25] Additionally, smart monitoring enables the extension of the operational life of appliances by reducing electronic waste and the carbon footprint associated with manufacturing new units,[26] which aligns with global sustainability goals.

While the AVF-SR framework provides robust diagnostic results, limitations must be addressed, such as intelligent fault detection according to manufacturing variations and differing usage patterns and manual labeling. Therefore, it is necessary to apply deep transfer learning and domain adaptation for cross-device monitoring. Additionally, self-supervised pretraining with unlabeled operational data needs to be considered to improve the framework's scalability. To ensure long-term, maintenance-free operation, energy-harvesting sensors also need to be integrated.

5. Conclusions

We developed and validated AVF-SR, which can be a high-performance solution for the intelligent monitoring of home appliances. The implementation of adaptive fusion and SR enabled significant improvements in the diagnostic reliability of the fault detection of home appliances. AVF-SR showed a 15 to 25% increase in accuracy through dynamic weight adjustment and elevated recognition rates from 65 to more than 85% in high-noise environments. By leveraging the complementary strengths of piezoelectric accelerometers for structural shocks and MEMS microphones for airborne signatures, AVF-SR provides a more effective method for diagnosing mechanical health than traditional single-sensor approaches. The diagnoses of bearing wear (a 0.85 confidence score), fan imbalance (a 0.72–0.78 confidence score), and start relay failure (a 0.78 confidence score) present the versatility of this multisensor integration.

The results of this study contribute to the development of a tool that simplifies complex signal processing and overcomes the constraints of consumer sensor technology. Multiscale wavelet decomposition to isolate frequency-specific anomalies (e.g., high-frequency bearing shocks vs low-frequency relay clicks) can be used for the development of smart sensors capable of edge-level diagnostic reasoning. The lightweight computation needed for AVF-SR enables the advanced condition monitoring for cost-sensitive, low-power microcontrollers. This can be applied to autonomous, self-diagnostic appliances that align with the requirements of the smart

home system. The results of this study contribute to the development of a sensor system that simplifies complex signal processing and overcomes the constraints of consumer sensor technology. However, it is necessary to reduce cross-brand generalization and data annotation costs. By adopting transfer learning and self-supervised models and emerging energy-harvesting technologies, the developed framework can be applied to large-scale industrial applications to form an autonomous and sustainable fault monitoring system for the smart home.

Acknowledgments

This research was supported by the High-Level Talent Research Start-up Funding Program of Xiamen Ocean Vocational College (Project Number KYG202537).

References

1 R. B. Randall: Vibration-based Condition Monitoring: Industrial, Aerospace and Automotive Applications. 2nd Edition (John Wiley & Sons, New Jersey, 2021) Chap. 4. https://doi.org/10.1002/9780470977668.ch4
2 G. D'Emilia and E. Natale: Int. J. Metrol. Qual. Eng. **12** (2021) 15. https://doi.org/10.1051/ijmqe/2021011
3 S. S. Vanraj and B. S. Pabla: Proc. 2018 Int. Conf. Condition Monitoring and Diagnosis (CMD, 2018) 1. https://doi.org/10.1109/CMD.2018.8535974
4 H. Jiang, Y. Wu, J. Yuan, Q. Zhao, and J. Chen: Sensors **24** (2024) 3762. https://doi.org/10.3390/s24123762
5 W. Zhang, X. Li, X. Jia, H. Ma, Z. Luo, and X. Li: Measurement **152** (2020) 107377. https://doi.org/10.1016/j.measurement.2019.107377
6 Q. Chen, S. Zheng, X. Wu, and T. Liu: Appl. Sci. **12** (2022) 10807. https://doi.org/10.3390/app122110807
7 C. S. Tu, C. K. Chiu, and M. T. Tsai: Appl. Sci. **14** (2024) 8229. https://doi.org/10.3390/app14188229
8 A. Orhan, N. Yordanov, M. Ertarğın, M. Zhilevski, and M. Mikhov: Machines **13** (2025) 737. https://doi.org/10.3390/machines13080737
9 Y. Haruna, S. Qin, A. H. A. Chukkol, A. A. Yusuf, I. Bello, and A. Lawan: Eng. Appl. AI **144** (2025) 110057. https://doi.org/10.1016/j.engappai.2025.110057
10 J. Xia, R. Huang, J. Li, Z. Chen, and W. Li: IEEE Trans. Instrum. Meas. **73** (2024) 1. https://doi.org/10.1109/TIM.2024.3417592
11 H. Omidvarborna, P. Kumar, J. Hayward, M. Gupta, and E. G. S. Nascimento: Atmosphere **12** (2021) 453. https://doi.org/10.3390/atmos12040453
12 Y. Liu, Y. Chai, Y. Mao, and A. Li: Proc. 44th Chinese Control Conf. (CCC, 2025) 8507. https://doi.org/10.23919/CCC64809.2025.11179004
13 Y. Han, S. Lv, Q. Huang, and Y. Zhang: Knowl.-Based Syst. **301** (2024) 112361. https://doi.org/10.1016/j.knosys.2024.112361
14 J. Ma, N. Li, Y. Jiang, and T. Feng: Int. J. Wire. Mob. Comput. **20** (2021) 201. https://dx.doi.org/10.1504/IJWMC.2021.115660
15 Z. Wang, D. Sun, K. Gong, W. Wang, and P. Sun: Electronics **10** (2021) 2679. https://doi.org/10.3390/electronics10212679
16 H. Zhu, X. Wang, Y. Zhao, Y. Li, and W. Wang: Proc. Inst. Mech. Eng. C: J. Mech. Eng. Sci. **229** (2014) 2303. https://doi.org/10.1177/0954406214557343
17 H. Liu, Y. Xu, Y. Qi, H. Yang, and W. Bi: Sensors **25** (2025) 3090. https://doi.org/10.3390/s25103090
18 V. R. Miranda and J. Landre Jr.: Int. J. Adv. Eng. Res. Sci. **5** (2018) 148. https://doi.org/10.22161/ijaers.5.11.21
19 C. Liu, Z. Shi, and T. Y. Hou: Sci. China Math. **60** (2017) 1733. https://doi.org/10.1007/s11425-016-9088-9
20 X. He and P. Niyogi: Proc. 17th Int. Conf. Neural Information Processing Systems (NeurIPS, 2003) 153. https://dl.acm.org/doi/10.5555/2981345.2981365
21 N. Kazeev, A. R. Al-Maeeni, I. Romanov, M. Faleev, R. Lukin, A. Tormasov, A. H. Castro Neto, K. S. Novoselov, P. Huang, and A. Ustyuzhanin: npj Comput. Mater. **9** (2023) 113. https://doi.org/10.1038/s41524-023-01062-z
22 A. C. de Oliveira, A. C. Lima Filho, F. A. Belo, and A. V. O. Cadena: Data **9** (2024) 106. https://doi.org/10.3390/data9090106

23 M. J. C. S. Reis, and A. J. D. Reis: Sensors **25** (2025) 4944. https://doi.org/10.3390/s25164944
24 Everyday Repair: https://everydayrepair.ca/appliance-repair-vs-replacement/ (accessed February 2026).
25 Hicron Software: https://hicronsoftware.com/blog/predictive-maintenance-in-automotive-warranty/ (accessed February 2026).
26 E. Cattermole: https://www.cattermoleelectrical.co.uk/why-repairing-instead-of-replacing-appliances-makes-a-big-difference (accessed February 2026).

About the Authors

Yuchao Zhao received his B.S. and M.S. degrees from Xiamen University, China, in 2002 and 2011, respectively. Since 2021, he has been a deputy director of the practice training center at Xiamen Ocean Vocational College. His main research interests are in the fields of electronics, communications, and intelligent manufacturing. (zhaoyuchao@xmoc.edu.cn).

Zhengji Mao received his B.S. and Ph.D. degrees from National Taiwan University, Taiwan, in 1986 and 1990, respectively. From 1996 to 2003, he was an associate professor at Nantai College of Technology. From 2004 to 2009, he was a professor at Taiwan Shoufu University. Since 2024, he has been a professor at Xiamen Ocean Vocational College. His research interests are in artificial intelligence, marine mechatronics, and automation sensors. (maozhengji@xmoc.edu.cn)